IOPscience iopscience.iop.org

Home Search Collections Journals About Contact us My IOPscience

Fragility, anharmonicity and anelasticity of silver borate glasses

This article has been downloaded from IOPscience. Please scroll down to see the full text article.

2006 J. Phys.: Condens. Matter 18 10915

(http://iopscience.iop.org/0953-8984/18/48/019)

View the table of contents for this issue, or go to the journal homepage for more

Download details:
IP Address: 129.252.86.83
The article was downloaded on 28/05/2010 at 14:42

Please note that terms and conditions apply.

INSTITUTE OF PHYSICS PUBLISHING JOURNAL OF PHYSICS: CONDENSED MATTER

J. Phys.: Condens. Matter **18** (2006) 10915–10929 doi:10.1088/0953-8984/18/48/019

Fragility, anharmonicity and anelasticity of silver borate glasses

Giovanni Carini[1], Giuseppe Carini[1], Giovanna D'Angelo[1], Gaspare Tripodo[1], Antonio Bartolotta[2] and Gaetano Di Marco[2]

[1] Dipartimento di Fisica, Università di Messina, Salita Sperone 31, I-98166 S Agata, Messina, Italy
[2] Istituto per i Processi Chimico-Fisici del CNR, Sezione di Messina, Via La Farina 237, I-98123 Messina, Italy

Received 10 April 2006, in final form 26 October 2006
Published 17 November 2006
Online at stacks.iop.org/JPhysCM/18/10915

Abstract

The fragility and the anharmonicity of $(Ag_2O)_x(B_2O_3)_{1-x}$ borate glasses have been quantified by measuring the change in the specific heat capacity at the glass transition temperature T_g and the room-temperature thermodynamic Grüneisen parameter. Increasing the silver oxide content above $X = 0.10$ leads to an increase of both the parameters, showing that a growing fragility of a glass-forming liquid is predictive of an increasing overall anharmonicity of its glassy state. The attenuation and velocity of ultrasonic waves of frequencies in the range of 10–70 MHz have also been measured in silver borate glasses as a function of temperature between 1.5 and 300 K. The experimental data reveal anelastic behaviours which are governed by (i) quantum-mechanical tunnelling below 20 K, (ii) thermally activated relaxations between 20 and 200 K and (iii) vibrational anharmonicity at even higher temperatures. Evaluation of tunnelling (C) and relaxation (C^*) strengths shows that C is independent of the structural changes affecting the borate network with increasing metal oxide content and is at least one order of magnitude smaller than C^*. The latter observation implies that only a small fraction of the locally mobile defects are subjected to tunnelling motions.

1. Introduction

The 'fragility' of a glass-forming liquid, a concept introduced by Angell [1, 2], is an important property which measures the thermal degradation of the glassy structure over the glass transition region by the departure from the Arrhenius behaviour of its viscosity η. It has been initially defined by the parameter $m = [\frac{\mathrm{d}\log\eta}{\mathrm{d}(T_g/T)}]_{T=T_g}$, that is the limiting slope of the viscosity curves at the glass transition temperature T_g; this permits us to place glass-forming liquids in the interval between the two extremes 'fragile' and 'strong', corresponding to the highest and the lowest value of m, respectively. 'Fragile' liquids, such as hydrated $Ca(NO_3)_2$ and *o*-terphenyl, are substances with non-directional interatomic or intermolecular

 © 2006 IOP Publishing Ltd Printed in the UK

bonds which permit drastic changes in local order at the glass transition leading to pronounced deviations from the Arrhenius behaviour for the viscosity. By contrast, 'strong' liquids (such as SiO_2 or GeO_2), characterized by strong covalent bonds which preserve the main structural characteristics over broad ranges of temperature, exhibit an Arrhenius dependence of the viscosity. A close correlation between transport behaviours and thermodynamic properties of glass-forming liquids has been also established [3, 4], fragile glass-formers exhibiting large excess heat capacities ΔC_p at T_g as opposed to small ΔC_p characterizing strong systems. According to these findings, the change in heat capacity ΔC_p at T_g represents an alternative evaluation of fragility.

A further important but poorly understood subject in glassy materials is the propagation of sound, mainly because many competing mechanisms are responsible for the behaviours observed in the different temperature and frequency ranges [5]. Low-energy defect states are responsible for anomalies in the acoustic attenuation and the sound velocity of glasses at low temperatures, exhibiting coherent or incoherent tunnelling effects below about 20 K [6] and thermally activated relaxations at higher temperatures [7]. Despite a large amount of experimental [8] and theoretical work [6, 9, 10], a consistent and convincing picture explaining the nature of low-energy excitations and accounting for the correlation existing between quantum-mechanical tunnelling and classical activation is still lacking.

Quite recently [11], it has been shown that the ultrasonic loss and the sound velocity of lithium borate glasses are mainly regulated by the contributions of tunnelling local motions below about 20 K and of thermally activated relaxations and the vibrational anharmonicity between 20 and 300 K. The results of that investigation emphasized that (i) differently from relaxing defects, tunnelling systems appear to be independent of structural changes characterizing a glassy network and (ii) the anharmonicity of a glass is closely correlated with the fragility of its liquid phase. We now extend this work to include silver borate glasses, with the aim of providing further data for investigating both the fragility behaviour and the relation between quantum tunnelling and classical activation in glasses. Vitreous B_2O_3 is a glassy prototype characterized by a connectivity (defined as the number of bridging oxygens per network forming ion (NFI)) of 3. The addition of silver oxide to B_2O_3 changes the network connectivity markedly, because it mainly assists the formation of charged $B\emptyset_4$ tetrahedral groups ($\emptyset$ = oxygen atoms bridging between two network forming boron ions) by crosslinks between the $B\emptyset_3$ planar groups building up the borate skeleton [12–15]. The concentration of $B\emptyset_4$ groups increases up to about $X = 0.20$ with a rate close to $R = X/(1 - X)$ [13], which corresponds to the formation of two $B\emptyset_4$ groups for each oxygen introduced by the metallic oxide. This leads to an increase of the connectivity from 3 up to 3.25 and to a stiffening of the structure, as proved by the marked increase in the elastic moduli [16]. Higher silver oxide contents ($X \geqslant 0.20$) cause the breaking of B–O–B linkages leading to growing numbers of non-bridging oxygens (NBO), occurring mainly in triangular BO_3 groups [17]; as a consequence, the coherence of the glassy network and the rate of increase of elastic moduli decline [16].

The paper is organized as follows. In section 2 we briefly describe the experimental details. In section 3 we present and discuss the experimental results of (i) specific heat capacity through the glass transition region, used to determine the composition behaviour of fragility in $(Ag_2O)_x(B_2O_3)_{1-x}$ glasses, (ii) linear thermal expansion coefficients between 100 and 350 K, used to determine the room-temperature thermodynamic Grüneisen parameters and (iii) ultrasonic attenuation and velocity between 1.5 and 300 K, used to determine the spectral densities of TLS (tunnelling or two-level systems) and of asymmetries Δ of double-well potentials schematizing the relaxing defects. In particular the experimental data will be analysed in the light of the theory, paying particular attention to the relation between anharmonicity and fragility and to the link between tunnelling states and relaxing defects $\gamma_{G,th}$.

Table 1. Room-temperature values of the density ρ, the velocities of longitudinal (v_l) and transverse (v_t) ultrasounds, the Debye temperature Θ_D, the adiabatic shear (G) and bulk (B) moduli, and the anharmonicity coefficient Γ_l in $(Ag_2O)_x(B_2O_3)_{1-x}$ glasses. The values of the glass transition temperatures T_g are also included.

Samples X	ρ (kg m^{-3})	T_g (K)	v_l (m s^{-1})	v_t (m s^{-1})	Θ_D (K)	G (GPa)	B (GPa)	Γ_l
0.0	1838	546	3367	1872	267	6.44	12.26	0.026
0.04	2109	575	3488	1929	279	7.85	15.19	0.021
0.09	2522	622	3885	2043	302	10.33	23.58	
0.14	2856	670	4176	2233	330	14.24	30.82	0.015
0.20	3193	697	4253	2249	332	16.15	36.22	0.016
0.25	3560	702	4353	2289	339	18.65	42.59	
0.33	3927	704	4314	2250	328	19.88	46.58	0.090

2. Experimental details

Glasses of the $(Ag_2O)_x(B_2O_3)_{1-x}$ system, where $0 \leqslant X \leqslant 0.33$, were prepared and characterized following the same specific procedures already described [11].

The specific heat capacities of the samples were determined using a Perkin Elmer differential scanning calorimeter (DSC-Pyris). Discs of each glass of mass approximately 15 mg were encapsulated in aluminium pans and subjected to the same thermal cycles: the as-quenched glasses were subjected to a first heating (from 300 K to about 650–780 K depending on their T_g) and subsequent cooling run, both at 20 K min^{-1}, followed by reheating at 20 K min^{-1}. The first run was necessary to erase the previous thermal history of as-quenched glasses, which causes effects of enthalpy recovery [18]. Calibrations of the DSC output were performed using a standard sapphire sample.

The attenuation and velocity of longitudinal and shear ultrasonic waves were measured between 1.5 and 300 K using a conventional pulse-echo ultrasonic technique in the 10–70 MHz frequency range.

Thermal expansion measurements were made from 100 K up to room temperature using a Netzsch Industries silica pushrod LVDT horizontal dilatometer with a heating rate of 2 K min^{-1}.

3. Experimental results and discussion

3.1. Thermal transitions and fragility

Figure 1(a) shows the heat capacity curves for selected $(Ag_2O)_x(B_2O_3)_{1-x}$ glasses, as typical. Above 300 K the specific heats of all the studied systems varied smoothly with increasing temperature, except for the usual endothermic peak at T_g which overlapped with a sudden jump from glassy to liquid-like behaviour through the glass transition temperature. The complete absence of melting endotherms in the explored temperature interval indicates that $(Ag_2O)_x(B_2O_3)_{1-x}$ glasses can be regarded as homogeneous amorphous systems. The T_g s of these borate glasses are reported in table 1 and, as expected [12], they increase with increasing Ag_2O content. As a measure of the fragility, we have chosen the dimensionless ratio between the variation ΔC_p ($=C_{p,l}-C_{p,g}$) of the specific heat capacity and $C_{p,l}$. $C_{p,l}$ and $C_{p,g}$ represent the specific heats in the liquid and glassy regions, respectively, where $C_{p,g}$ corresponds to the value of C_p at about 100 K below the temperature of the endothermic peak. The values of $\frac{\Delta C_p}{C_{p,l}}$

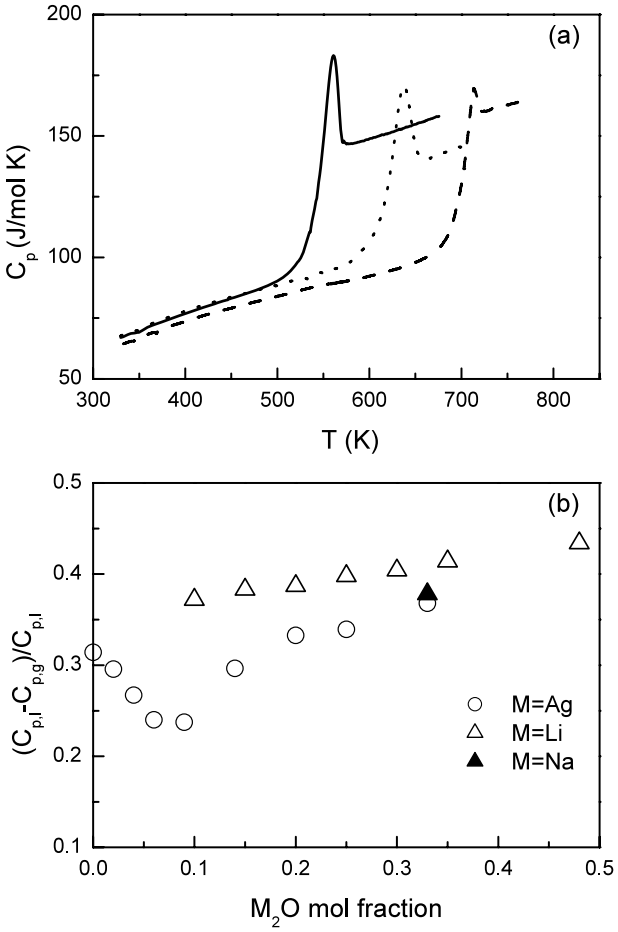

Figure 1. (a) Temperature variation of the heat capacity in $(Ag_2O)_x(B_2O_3)_{1-x}$ glasses obtained by DSC at a scan rate of 20 K min^{-1}: $X = 0.0$, solid line; $X = 0.09$, dotted line; $X = 0.25$, dashed line. (b) Compositional dependence of $\frac{\Delta C_p}{C_{p,l}}$ in $(M_2O)_x(B_2O_3)_{1-x}$ borate glasses: present results for M = Ag, (○); data for M = Li (△) and M = Na (▲), taken from [18].

obtained with increasing Ag_2O concentration are reported in figure 1(b) and show a minimum at $X \sim 0.1$ followed by a monotonic increase for higher concentrations.

According to Angell's classification scheme [3, 19], B_2O_3 is quite a strong glass-former having a fragility of $m = 32$; as a consequence, silver borate systems are strong glass-formers which become increasingly fragile as the silver oxide content increases above $X = 0.1$. A similar trend has been also revealed in $(Li_2O)_x(B_2O_3)_{1-x}$ glasses over the concentration range $0.1 \leqslant X \leqslant 0.5$ [18] and the $\frac{\Delta C_p}{C_{p,l}}$ values (taken at a heating rate of 10 K min^{-1}) are also included in figure 1(b) for comparison. Unfortunately data for the specific heat capacity for concentrations of lithium oxide lower than $X = 0.1$ are not available, preventing the possible observation of a minimum in the fragility behaviour as determined by calorimetry. It is worth noting, however, that a minimum at $X \sim 0.08$ has been revealed in the fragility behaviour of lithium borate systems, also determined by calorimetric techniques [20]; in this case, the fragility has been evaluated by considering the ratio between T_g and the width ΔT of the temperature interval over which the calorimetric glass transition takes place.

The structural mechanism driving the decrease (for $X < 0.1$) and the next increase (for $X > 0.1$) of fragility in these silver borate systems could be explained in terms of changes altering the short- and medium-range structure of the borate network when the glass liquefies crossing the glass transition region. The effect of temperature on sodium, potassium and lithium borate glasses has been investigated by NMR [21], high temperature Raman spectroscopy [22] and molecular dynamics studies [23]. These investigations proved that, in alkali borate glasses $(M_2O)_x(B_2O_3)_{1-x}$ with $X \geqslant 0.20$, increasing temperature above T_g causes a decrease of $B\emptyset_4$ tetrahedral groups which transform into triangular BO_3 groups containing one or two NBOs in agreement with the following isomerization reactions [23]: $[^{(-)}\emptyset_3B\text{–}\emptyset\text{–}B\emptyset_2] \leftrightarrow [B\emptyset_2O^{(-)} + B\emptyset_3]$ and $[^{(-)}O\emptyset B\text{–}\emptyset\text{–}B\emptyset O^{(-)}] \leftrightarrow [^{(2-)}O_2B\text{–}\emptyset\text{–}B\emptyset_2]$. The former implies the transformation of charged tetrahedral groups into charged borate triangles with one NBO and the latter the transformation of linked charged borate triangles containing one NBO each in linked borate triangles, one of them with two NBOs (doubly charged). The metallic cations occupy specific positions within the different anionic environments of the host structure in order to preserve the electrical neutrality. Therefore, it is believed that, for a Ag_2O content lower than $X \sim 0.1$, the formation of BO_4 groups strengthens the borate network which remains quite stable also in the melt. The construction of the four-coordinated borate network in the glassy state continues to proceed for $X > 0.1$, but to the detriment of its chemical stability [18]. This is recovered in the liquid state by the isomerization reactions which retransform $B\emptyset_4$ groups in triangular BO_3 groups containing one or two NBOs. The collapse of the four-coordinated network gives rise to supplementary degrees of freedom: the increasing jumps ΔC_p of the specific heat capacity observed at T_g for $X > 0.1$ could be associated with these changes which give rise to increasing variations of the configurational entropy. This explanation is also consistent with the smaller fragility exhibited by (Ag_2O)–(B_2O_3) systems when compared to (Li_2O)–(B_2O_3) systems. In fact, improved NMR spectroscopy measurements [24] revealed that, among alkali borate glasses having corresponding compositions, the fraction of BO_4 groups decreases as the alkali cation size increases, lithium borates being characterized by the largest fractions of these groups. Therefore this finding should account for the higher value of ΔC_p of lithium borate when compared to that of sodium borate glass [18], also reported in figure 1(b), because a larger excess of additional degrees of freedom is expected from a larger number of fragmented BO_4 groups. Unfortunately, the same refined analysis has not been extended to silver borate glasses for which only quite old NMR data exist [13]. Assuming, however, that the trend revealed in alkali borate glasses is also valid for silver borates, the smaller proportion of BO_4 groups expected in silver borates when compared to lithium borates should lead to lower values of ΔC_p, as observed.

3.2. Thermal expansion and anharmonicity

Figure 2(a) shows the temperature dependence of the linear thermal expansion coefficient α_{th} of selected silver borate glasses. Above 100 K, $\alpha_{th}(T)$ increases linearly with temperature with about the same slope for all the studied glasses. The room-temperature values of α_{th}, compared with those of lithium borate glasses [11, 25] in figure 2(b), show a well-defined minimum at $X = 0.20$, characteristic also of alkali borate glasses [25]. This is attributed to the competition between the two main structural mechanisms, the formation of $B\emptyset_4$ groups and (for $X \geqslant 0.20$) of NBOs, driving the expansion of the glassy network in two opposite directions. The former increases the connectivity of the network leading to tighter structures having smaller thermal expansion coefficients, while the latter introduces weak links favouring the expansion capability. In order to have more insight into the composition behaviour of the anharmonicity, the room-temperature coefficients α_{th} have been combined with the adiabatic

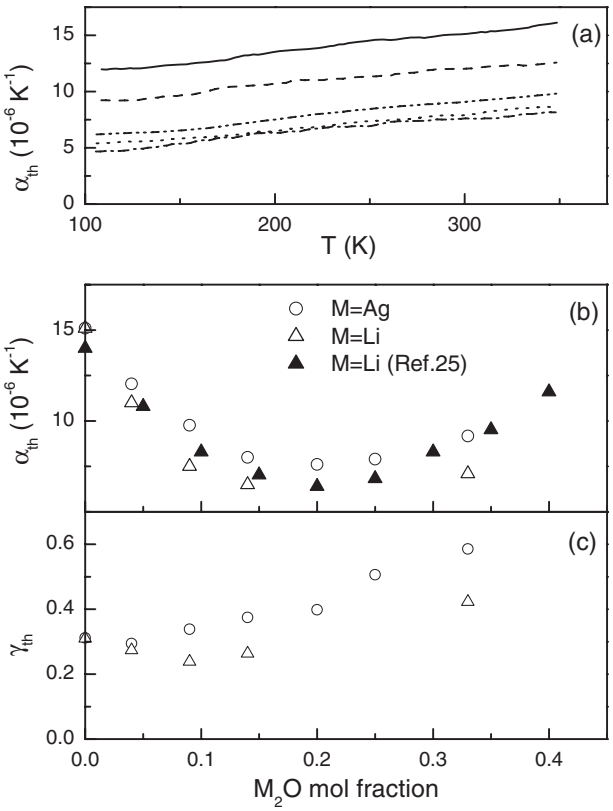

Figure 2. (a) Temperature dependence of the linear thermal expansion coefficient in $(Ag_2O)_x(B_2O_3)_{1-x}$ glasses: $X = 0.0$, solid line; $X = 0.04$, dashed line; $X = 0.14$, dotted line; $X = 0.20$, dashed–dotted line; $X = 0.33$, dashed–double dotted line. (b) Compositional dependence of the linear thermal expansion coefficient in $(M_2O)_x(B_2O_3)_{1-x}$ glasses: present results for M = Ag (○) and M = Li (△); data for M = Li (▲), taken from [25]. (c) Comparison between the compositional dependences of the thermal Grüneisen parameter $\gamma_{G,th}$ in $(M_2O)_x(B_2O_3)_{1-x}$ glasses: M = Ag, (○); M = Li, (△).

bulk modulus B^S, the molar volume V_m and the molar heat capacities at constant pressure C_p in order to obtain the thermodynamic Grüneisen parameter $\gamma_{G,th} = \frac{3\alpha_{th}B^T V_m}{C_V} = \frac{3\alpha_{th}B^S V_m}{C_p}$. In this relation, C_V is the molar heat capacity at constant volume and B^T the isothermal bulk. The elastic parameters determined at ultrasonic frequencies in the present study are the adiabatic bulk ($B^S = \rho V_l^2 - \frac{4}{3}G^S$) and shear ($G^S = \rho V_t^2$) moduli; in the following and in the tables, they will be referred to as B and G. A quasi-harmonic solid can be considered as a set of harmonic oscillators having frequencies which are volume dependent; each oscillator has a modal Grüneisen parameter given by [26]:

$$\gamma_{G,i} = -\frac{d(\ln \omega_i)}{d(\ln V)}$$

where ω_i is the frequency of the ith mode. The thermodynamic Grüneisen parameter is then obtained by summing over these modes:

$$\gamma_{G,th} = \frac{\sum C_i \gamma_{G,i}}{\sum C_i}$$

where each $\gamma_{G,i}$ is weighted by the heat capacity C_i of the mode. Thus $\gamma_{G,th}$ includes the contributions from all the vibrational modes and is a convenient parameter for analysing the effects of anharmonicity. The estimated $\gamma_{G,th}$ are compared with those of lithium borate glasses [11] in figure 2(c): the values are small and range between 0.2 and 0.6, as commonly observed in a number of glasses. Tetrahedrally bonded SiO_2 and GeO_2 [27], vitreous As_2S_3 [27], sodium silicate [28] and Ge–Se [29] glasses have room-temperature $\gamma_{G,th}$ values ranging between 0 and 1. Low values of $\gamma_{G,th}$ imply the presence of vibrational modes having small or negative γ_i. In fact, ultrasonic measurements under pressure on silver borate glasses [30] revealed that, in clear contrast with the positive values determined for the longitudinal acoustic-mode Grüneisen parameter $\gamma_{G,l}$ (X), the shear acoustic-mode $\gamma_{G,t}$ (X) are negative; as a consequence, the mean acoustic-mode Grüneisen parameters $\gamma_{G,el}$ (X) in the long-wavelength elastic limit are still positive, but very small. In vitreous SiO_2 both the longitudinal and shear acoustic-mode Grüneisen parameters are negative: the presence of vibrational modes having negative γ_i has been explained by considering the open structure of this glass which allows bending vibrations of oxygens bridging between two silicon atoms [31]. This model emphasizes the importance of low-frequency transverse vibrations whose frequency increases with increasing volume. The low values of $\gamma_{G,th}$ (X) imply that bending vibrations could also play a significant role in the vibrational anharmonicity of silver borate glasses.

Since the anharmonicity of solids is too complex an argument to be described adequately by a single parameter, we would like to remark that the following considerations must be regarded as highly tentative. In terms of a highly simplified view, the compositional dependence of $\gamma_{G,th}$ (X) can be explained by considering the structural changes caused by network modifier ions (NMI) to the borate network. For $X < 0.1$, the formation of $B\emptyset_4^-$ groups stiffens and tightens the system, giving rise to a significant reduction in the thermal expansion coefficient. With increasing Ag_2O concentration, the anharmonic rattling of Ag^+ modifier ions within their local cages affects markedly the motion of $B\emptyset_4^-$ groups and (for $X \geqslant 0.2$ [13, 24]) of NBOs as a consequence of Coulombic interactions which cause restoring forces for the motion of oxygen atoms. The restoring forces increase the bulk modulus of the whole network with increasing silver concentration and enhance the expansion capability of the vibrational modes following the short-time motions of Ag^+ ions in asymmetric binding potentials determined by their Coulombic interactions with oxygen atoms. In addition to this, for concentrations higher than $X \sim 0.20$, NBOs tend to soften the borate network, giving rise to the formation of weak links and favouring the enhancement of the expansion coefficient. These two mechanisms work in competition with the network tightness due to $B\emptyset_4^-$ groups, resulting in an overall larger anharmonicity of the vibrational modes for $X > 0.10$. In this context, the smallest values of $\gamma_{G,th}$ (X) characterizing lithium borate glasses account for the highest cation field strength of Li^+ ions (1.88 $Å^{-2}$) when compared to that of Ag^+ ions (0.77 $Å^{-2}$). The cation field strength q/r^2, given by the ratio between the formal charge q of the ion and the squared ionic radius r, has been evaluated using the values of r reported by Shannon [32] for the coordination numbers estimated by neutron diffraction experiments ($N_{Li–O} = 4.1 \pm 0.5$ and $N_{Ag–O} = 3.7 \pm 0.5$, [15]). It is believed that the highest field strength constrains Li^+ ions within less asymmetric binding potentials, limiting the amplitude of their short-time motion and the overall expansion capability of the network.

Finally we would like to emphasize that the variation with composition of $\gamma_{G,th}$ in silver and lithium [11] borate glasses is qualitatively similar to that of fragility, showing that the addition of metal oxide drives the system towards a structure which is less resistant to the thermal degradation of its molecular aggregation, as a consequence of a larger expansion capability of the vibrations. These observations imply that the fragility regulating the dynamics of a glass-forming liquid at the glass transition could play a significant role in determining the

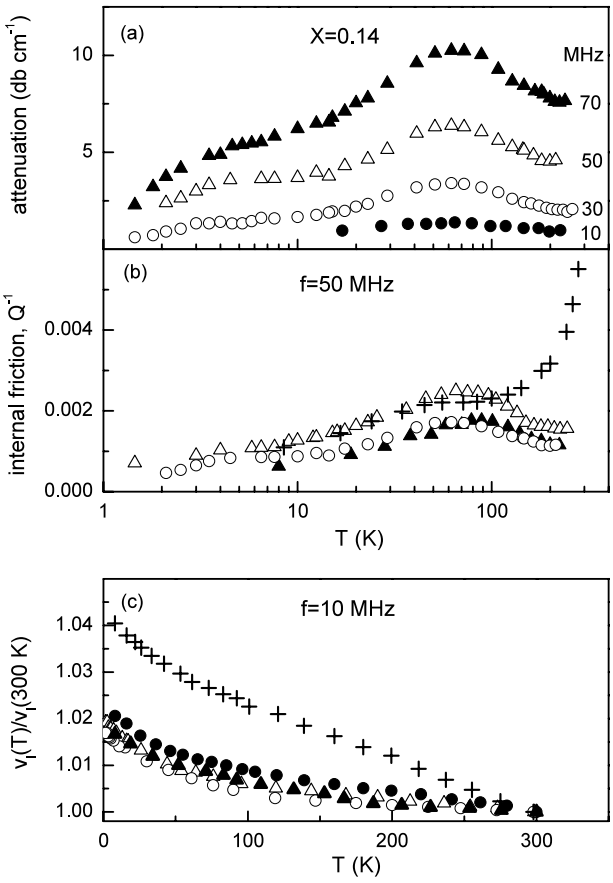

Figure 3. (a) The temperature dependence of the attenuation of longitudinal ultrasonic waves at selected driving frequencies in $(Ag_2O)_{0.14}(B_2O_3)_{0.86}$ glass. (b) The effect of silver ion concentration on the temperature dependence of the internal friction Q^{-1} of 50 MHz longitudinal ultrasonic waves in $(Ag_2O)_x(B_2O_3)_{1-x}$ glasses: $X = 0.04$, (Δ); $X = 0.14$, (○); $X = 0.20$, (▲); $X = 0.33$, (+). (c) Temperature dependence of the fractional sound velocity $\frac{V_l(T)}{V_{l,\mathrm{rt}}}$ of 10 MHz longitudinal ultrasonic waves in $(Ag_2O)_x(B_2O_3)_{1-x}$ glasses: $X = 0.0$, (●); $X = 0.04$, (Δ); $X = 0.14$, (○); $X = 0.20$, (▲); $X = 0.33$, (+).

anharmonicity of the resulting glass. 'Fragile' as opposed to 'strong' glass-formers should have an overall larger anharmonicity regulating their vibrational properties.

3.3. Ultrasonic attenuation: tunnelling and relaxations

The temperature dependence from 1.5 to 300 K of the attenuation of longitudinal ultrasonic waves in $(Ag_2O)_{0.14}(B_2O_3)_{0.86}$ glass at selected frequencies is shown in figure 3(a), as typical of the studied glasses. As the temperature is increased from 1.5 K the attenuation rises until it reaches a plateau which extends up to about 10 K. Above this region the attenuation increases up towards a broad peak, whose maximum shifts to higher temperatures as the ultrasonic driving frequency is increased. These observations imply that, in the temperature range above about 20 K, the acoustic behaviours are governed by thermally activated relaxations of structural defects, characterized by a distribution of relaxation times τ as a consequence of

the inherent randomness of the glassy topology. Increasing the Ag_2O concentration leads to a decrease of the relaxation peak, as shown in figure 3(b) which shows the internal friction Q^{-1} ($=0.23\alpha_{db}v/\omega$, where α_{db} is the attenuation in db cm^{-1}, v the sound velocity and ω the angular frequency) of 50 MHz longitudinal waves for $(Ag_2O)_x(B_2O_3)_{1-x}$ glasses. In particular, the glass with $X = 0.33$ exhibits a loss peak which merges into the low-temperature tail of a sharp increase of attenuation due to the ionic migration peak, whose maximum is located at about 400 K in the MHz frequency range [33]. This glass, in fact, is a good ionic conductor and is used as main component for synthesizing a class of vitreous fast ionic conductors [33]. We do not give the attenuation for shear waves, except to report that over the whole temperature range explored the internal friction was found to be about the same as that for longitudinal waves, as found also [11, 34] for alkali borate glasses.

The explored frequency range is quite limited and enables us only to get rough evaluation of the average activation energy E_{act} and the characteristic frequency τ_0^{-1} of the relaxation process. The Arrhenius plot of the frequencies versus the reciprocal temperatures of the acoustic loss maxima gives values of E_{act}/k_B and τ_0^{-1} for $(Ag_2O)_x(B_2O_3)_{1-x}$ glasses, which are close to about 700 K and 10^{13} s^{-1}, respectively.

To analyse quantitatively the temperature dependence of the ultrasonic internal friction Q^{-1} of silver borate glasses we will follow the same lines already discussed in a very recent paper [34], where the relaxation processes were described by the asymmetric double-well potential (ADWP) model [35, 36]. Since the tunnelling model is also based on asymmetric double-well potentials, application of the ADWP model permits a connection between tunnelling and classical activation, because for both mechanisms the ultrasonic strain interacts with the defect states by modulation of the asymmetry Δ. Therefore only a short account of the theoretical approaches explaining the experimental data will be given in the following.

The low-temperature plateau of internal friction, whose onset shifts to higher temperatures with increasing frequency (see figure 3(a)), has been explained in terms of phonon-assisted tunnelling of two-level systems and is directly related to the tunnelling strength C_i [37]:

$$Q^{-1}_{i,\text{plateau}} = \frac{\pi}{2}\left[\frac{\bar{P}\gamma_i^2}{\rho V_i^2}\right] = \frac{\pi}{2}C_i. \tag{1}$$

Here V_i is the ultrasonic wave velocity, γ_i the deformation potential that expresses the coupling between the ultrasonic stress and the system, $\bar{P}$ the TLS spectral density, ρ the sample density, while the index i refers to the different polarizations (l stands for longitudinal and t for transverse). A background of ultrasonic attenuation, which is temperature independent but frequency dependent, has been discarded using the procedure described in detail in [38]. The calculated values of the product $\bar{P}\gamma_i^2$ increase with increasing Ag_2O concentration (table 2), a trend which mainly reflects the growth of the deformation potential γ_l. The deformation potentials for silver borate glasses were deduced by linear interpolation from the plot of the values of γ_l, experimentally determined in lithium borate glasses [39], versus the corresponding glass transition temperatures T_g [40]. The resulting TLS spectral density $\bar{P}$ does not show any definite variation with increasing Ag_2O concentration. It is also worth noting that the longitudinal tunnelling strengths C_l show a magnitude ranging between 10^{-3} and 10^{-4}, as universally observed in almost all the glasses [8].

With increasing temperature above the region of the plateau, the internal friction rises and, at still higher temperatures, exhibits a maximum associated with thermally activated relaxations of structural defects over the potential barriers. A contribution to the increase of Q^{-1} between about 8 and 20 K, i.e. the region between the plateau and the loss peak, can arise from incoherent tunnelling effects within the two wells as a consequence of increasing thermal

Table 2. Values of the parameters related to the phonon-assisted tunnelling (C_1, $\bar{P}\gamma_1^2$, γ_1, $\bar{P}$) and to the thermally activated relaxation (C_1^*, V_0, τ_0, and $f_0\gamma_1^2$ and f_0) in $(Ag_2O)_x(B_2O_3)_{1-x}$ glasses.

Samples X	C_1 (10^{-4})	$\bar{P}\gamma_1^2$ (10^7 J m^{-3})	γ_1 (eV)	$\bar{P}$ (10^{45} J^{-1} m^{-3})	C_1^* (10^{-3})	$f_0\gamma_1^2$ (10^8 J m^{-3})	f_0 (10^{46} J^{-1} m^{-3})	V_0/k_B (K)	τ_0 (10^{-14} s)
0.0	2.4[a]	0.52[a]	0.21	4.5[a]	8.28	1.73	15.3	725	9.6
0.04	6.93	1.78	0.34	6.0	17.2	4.41	14.86	893	2.9
0.11	4.83[b]	1.93[b]	0.5	3[b]					
0.14	5.2	2.59	0.57	3.1	15.3	7.62	9.14	740	6.18
0.20	3.97[b]	2.46[b]	0.64	2.4[b]	14.14	8.17	7.77	924	5.4
0.33	5.68[b]	4.47[b]	0.65	4.1[b]					

[a] Values taken from [39].
[b] Values taken from [38].

motion which prevents the phase coherence of TLS tunnelling motion [6]. Limiting the present analysis to the temperature region above 20 K where only the relaxation process is dominant, the loss peak can be described by the ADWP model following the procedure described by Gilroy and Phillips (GP) [36]. In the GP framework, barrier heights V varying randomly over the defect sites with an exponential distribution, $g(V) = V_0^{-1}\exp(-\frac{V}{V_0})$, and asymmetries Δ having a constant distribution, $f(\Delta) = f_0$, have been used. In the model, the relaxation time τ of the process has been approximated by the usual Arrhenius law, $\tau = \tau_0 e^{V_0/k_B T}$, where the average activation energy is the parameter V_0 of the distribution and the characteristic time τ_0 is related to the vibrational frequency of the relaxing defect in a single well. This gives the following expression which accounts for the temperature dependence of the acoustic loss with an error of a few per cent in the ultrasonic range [36]:

$$Q_{i,\mathrm{rel}}^{-1} = \pi\left(\frac{f_0\gamma_i^2}{\rho V_i^2}\right) a\,(\omega\tau_0)^a = \pi C_i^* a(\omega\tau_0)^a. \tag{2}$$

In equation (2) C^* is the relaxation strength, $a = \frac{k_B T}{V_0} = \frac{T}{T_0}$ and the other parameters are defined above. The values of C_1^*, V_0 and τ_0^{-1} obtained by numerical evaluation of the experimental data are reported in table 2 and a typical fit of the relaxation loss, reproducing quite well the shape of the experimental results, is shown by a solid line in figure 4(a). It should be pointed out that similar fits have been carried out also by using a constant distribution of asymmetries f_0 and a Gaussian distribution for $g(V)$, but agreement with the experiment was then not so good as that obtained by using the exponential distribution, as already observed [34].

Figure 5(a) shows an important result of the present analysis: *the relaxation strength C_1^* is found to be more than one order of magnitude larger than the tunnelling strength C_1*.

From the values of C_1^* we have deduced the spectral density of asymmetries f_0, which decreases with increasing Ag_2O concentration from 15.3×10^{46} J^{-1} m^{-3} in pure B_2O_3 to 7.7×10^{46} J^{-1} m^{-3} in the glass with $X = 0.20$ (see table 2). According to a previous evaluation [34], an order of magnitude of 10^{26} m^{-3} has been obtained for the number of relaxing particles which also decreases by going from pure B_2O_3 to $(Ag_2O)_{0.20}(B_2O_3)_{0.80}$ glass. This excludes a significant contribution of OH^- impurities to the relaxation losses [11], because FTIR (Fourier transform IR) analysis of the glasses studied here revealed no sign of these extrinsic defects within experimental accuracy. In addition to the decreasing density of relaxing defects, there is an apparent activation energy V_0 which does not show any definite variation with increasing Ag_2O concentration. It is considered that the latter feature should be attributed to relaxing particles whose local arrangement is not greatly influenced by structural modifications induced by network modifier ions. The absence of an adequate

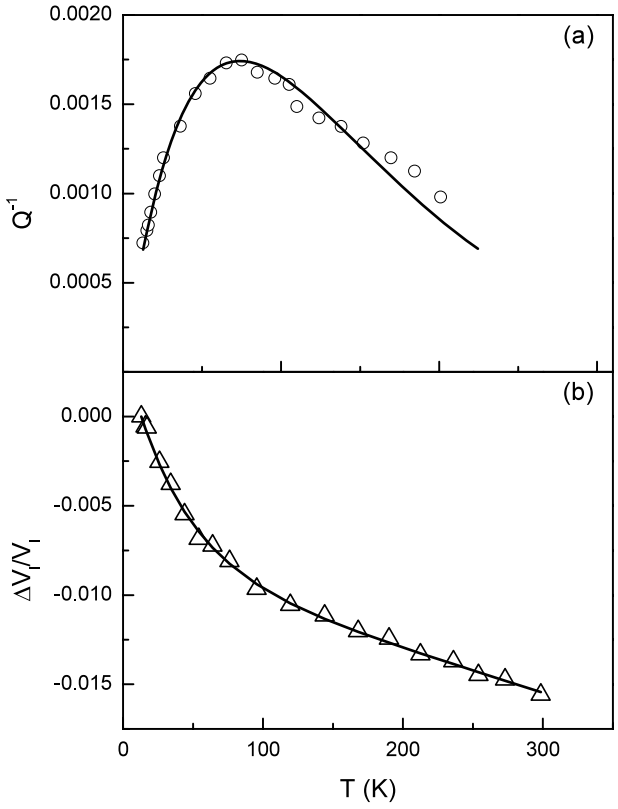

Figure 4. (a) Comparison between the experimental data for the internal friction at 50 MHz across the broad relaxation peak in $(Ag_2O)_{0.04}(B_2O_3)_{0.96}$ glass and the theoretical fits with the exponential distribution of activation energies (continuous line). (b) Comparison between the temperature dependence of the fractional sound velocity of 10 MHz longitudinal ultrasonic waves in $(Ag_2O)_{0.04}(B_2O_3)_{0.96}$ glass and the theoretical curve (continuous line) obtained by the relaxation and anharmonic contributions evaluated using equations (4) and (5), respectively.

model to describe the microscopic nature of defect states in glassy B_2O_3 led us to try a possible explanation for the observed anelastic effects. Both the findings involving $f(\Delta)$ and V_0 could be considered as an indication of structural relaxations which originate from some kind of local motion of $B\emptyset_3$ groups building up the borate network. Since the addition of silver oxide converts $B\emptyset_3$ groups to $B\emptyset_4^-$ tetrahedrons and (for $X \geqslant 0.20$) $B\emptyset_2O^-$ triangles, Coulombic interactions between Ag^+ cations and these charged groups, leading to a reduction of their degrees of freedom and of their local mobility, are expected. These additional interactions could represent the source for the observed decrease of the number of relaxing units. In this context, a larger cation field strength should be more efficient in reducing the number of relaxing particles. Numerical evaluation of the relaxation strength C_1^* of the loss peaks observed in $(Li_2O)_{0.04}(B_2O_3)_{0.96}$ and $(Li_2O)_{0.14}(B_2O_3)_{0.86}$ glasses [11] leads to values of f_0 (9.6×10^{46} J^{-1} m^{-3} and 3.7×10^{46} J^{-1} m^{-3}, respectively) that are significantly smaller than those obtained in silver borate glasses having the same molar ratios (see figure 5(b)).

Comparison between the tunnelling strength C_1 and the relaxation strength C_1^* (figure 5(a)), quantities determined quite directly by the experimental data, and between the spectral densities $\bar{P}$ and f_0 (figure 5(b)), reveal differences of more than one order of magnitude. Furthermore the

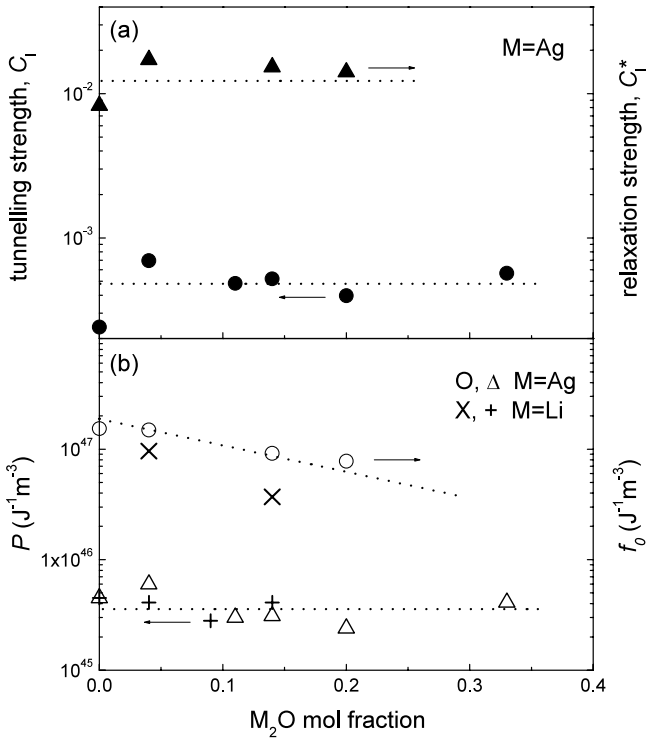

Figure 5. (a) Comparison between the tunnelling (●) and relaxation (▲) strengths of $(Ag_2O)_x(B_2O_3)_{1-x}$ glasses. The dotted lines are only guides for the eye. (b) Comparison between the spectral densities of TLS ($\bar{P}$) and asymmetries (f_0) of $(M_2O)_x(B_2O_3)_{1-x}$ glasses. The dotted lines are only guides for the eye.

slight oscillation in $\bar{P}$ with increasing Ag_2O and Li_2O (values taken from [11]) concentration contrasts with the clear-cut decrease observed for f_0. If the same microscopic origin drives tunnelling effects and classical activation [6], the above differences imply that only a fraction of the relaxing centres experiences tunnelling motion.

A further consideration results from the close similarity between the concentration behaviours of both f_0 and α_{th} up to $X = 0.20$. This implies that the Coulombic interactions between NMIs and the charged $B\emptyset_4^-$ tetrahedrons impose severe restrictions on the expansion capability of the network and its thermally activated local mobility. The present observations lead to the conclusion that glasses having a structure modified by increasing NMI addition leave the TLS density almost unaltered, confirming once more their universal nature as inherent to the glassy state, but alter the thermally activated local mobility substantially.

3.4. Sound velocity: relaxations and vibrational anharmonicity

In figure 3(c), the temperature variations of the sound velocity v_l of 10 MHz longitudinal waves in $(Ag_2O)_x(B_2O_3)_{1-x}$ glasses are reported as $v_l(T)/v_{l,rt}$, $v_{l,rt}$ being the value at room temperature. There is a continuously changing slope for temperatures varying in the interval between about 2 and 100 K and a nearly linear trend for higher temperatures. The decrease observed at temperatures between 10 and 100 K becomes increasingly smaller with increasing concentration up to $X = 0.20$, while the slope of the linear behaviour above 100 K decreases

by going from pure B_2O_3 to $(Ag_2O)_{0.14}(B_2O_3)_{0.86}$ and then increases with growing silver ion concentration.

As already observed in alkali borate glasses [11, 34], the sound velocities of silver borate glasses decrease with increasing temperature in the whole investigated range, but exhibit a larger slope at low temperatures. With respect to dynamical mechanisms driving the temperature behaviour of the sound velocity, we can distinguish three different regimes: (i) quantum mechanisms having TLSs as mainly responsible between 1.5 and 20 K, (ii) thermally activated relaxations causing the significant drop observed between 20 and 120 K and (iii) the vibrational anharmonicity regulating the nearly linear trend at even higher temperatures. The temperature dependence of the variation of longitudinal sound velocity V_l in the range between 20 and 300 K can be expressed well by [34]:

$$\left(\frac{\Delta V_l}{V_{l,0}}\right) = \left(\frac{\Delta V_l}{V_{l,0}}\right)_{\text{rel}} + \left(\frac{\Delta V_l}{V_{l,0}}\right)_{\text{anh}} \tag{3}$$

where $\Delta V_l = V_l(T) - V_{l,0}$ and $V_{l,0}$ is the sound velocity at the lowest temperature in the experiment.

In the right-hand side of equation (3) the relaxation term is given by [36]:

$$\left(\frac{\Delta V_l}{V_{l,0}}\right)_{\text{rel}} = \left(\frac{f_0 \gamma_l^2}{\rho V_l^2}\right)\left[(\omega\tau_0)^{\alpha} - 1\right] = C_l^*\left[(\omega\tau_0)^{\alpha} - 1\right] \tag{4}$$

and the anharmonic term by [41, 42]

$$\left(\frac{\Delta V_l}{V_{l,0}}\right)_{\text{anh}} = \left(\frac{L}{L_0}\right)^{\frac{3}{2}}\left[1 - \Gamma_l F\left(\frac{T}{\Theta}\right)\right]^{\frac{1}{2}} - 1 \tag{5}$$

where L is the length of the sample, L_0 the length of the sample at $T = 0$ K and Θ the Debye temperature. $F(\frac{T}{\Theta})$ is the usual function determining the internal energy of a Debye solid and the anharmonicity coefficient Γ_l, a dimensionless parameter mainly depending on the mean acoustic-mode Grüneisen parameter $\gamma_{G,el}$, has been assumed to be temperature independent [11, 34].

Using the parameters obtained by the numerical evaluation of the relaxation loss (table 2) in equation (4) and the room-temperature values of Θ (table 1) in equation (5), the temperature behaviours of the sound velocity have been evaluated by using Γ_l as the only parameter of the fit. The values of Γ_l are reported in table 1 and a typical fit of $(\frac{\Delta V_l}{V_{l,0}})$ is shown by a continuous line in figure 4(b). Γ_l decreases with increasing concentration showing a minimum in the range between $X = 0.14$ and $X = 0.20$ and then a sharp increase at $X = 0.33$. The concentration behaviour of Γ_l appears to reflect that of α_{th}, which shows a well-defined minimum at $X \sim 0.2$ (figure 2(b)).

4. Conclusions

Silver and lithium borate glasses represent good model systems for investigating the relations existing between (i) fragility and anharmonicity and (ii) quantum tunnelling effects and classical activation. Increasing addition of metal oxide leads to controlled variations of the elementary structural groups building up the borate network, permitting us to get useful information on the microscopic origin of the observed behaviours. The observed increase of fragility with increasing metal oxide content has been interpreted in terms of isomerization reactions which transform $B\text{Ø}_4$ groups into triangular BO_3 groups containing one or two NBOs with increasing temperature over the glass transition region. The parallel enhancement of the anharmonicity of the glass, as estimated by the room-temperature Grüneisen parameter, implies

that metal cations have a stronger temperature dependence of the vibrational amplitudes than the rest of the host borate network as a consequence of their anharmonic rattling within their local cages. To the extent to which this simple picture describes appropriately the role of cations, it is tentatively suggested that they drive the system towards a structural configuration which is less resistant to thermal degradation as the temperature is increased to and above T_g, probably triggering the discussed isomerization reactions.

The acoustic attenuation and the sound velocity show temperature behaviours over the range between 1.5 and 300 K mainly governed by localized motions of structural defects and by the anharmonicity. The locally mobile particles experience quantum tunnelling motions below 10 K and classical activation over potential barriers above 20 K. The tunnelling strength C_l ranges between 10^{-4} and 10^{-3} for both silver and lithium borate glasses and is found to be independent of the structural changes of the borate network. The relaxation strength C_l^*, however, is found to be of the order of 10^{-2} and exhibits a well-defined decrease with increasing metal oxide content which causes a significant reduction of the triangular $B\emptyset_3$ groups building up the skeleton of boron dioxide. Despite the lack of an adequate microscopic model describing the low-energy excitations in borate glasses, these observations lead us to associate the defect states with some kind of local motion of $B\emptyset_3$ groups within the borate network, also revealing that only a small fraction of relaxing particles are involved in tunnelling local motions below 10 K. The totality of observations lead to the conclusion that, differently from thermally activated relaxing centres, TLS spectral density is largely independent of the morphology of an amorphous solid, confirming its universal nature as intrinsic to the glassy state.

References

[1] Angell C A 1984 *Relaxation in Complex Systems* ed K Ngai and G B Wright (Washington, DC: Office of Naval Research) p 3
[2] Angell C A 1995 *Science* **267** 1924
[3] Angell C A 1991 *J. Non-Cryst. Solids* **131–133** 13
[4] Tatsuminago M, Halfpap B L, Green J L, Lindsay S M and Angell C A 1991 *Phys. Rev. Lett.* **64** 1549
[5] Fabian J and Allen P B 1999 *Phys. Rev. Lett.* **82** 1478
[6] Rau S, Enss C, Hunklinger S, Neu P and Würger A 1995 *Phys. Rev.* B **52** 7179
[7] Hunklinger S and von Schickfus M 1981 *Amorphous Solids* vol 24, ed W A Phillips (Berlin: Springer) p 81
[8] Pohl R, Liu X and Thompson E 2002 *Rev. Mod. Phys.* **74** 991
[9] Coppersmith S N 1991 *Phys. Rev. Lett.* **67** 2315
[10] Parshin D A 1994 *Phys. Rev.* B **49** 9400
Parshin D A 1994 *Phys. Solid State* **36** 991
[11] Carini G Jr, Carini G, D'Angelo G, Tripodo G, Bartolotta A and Salvato G 2005 *Phys. Rev.* B **72** 14201
[12] Boulos E N and Kreidl N J 1971 *J. Am. Ceram. Soc.* **54** 368
[13] Kim K S and Bray P J 1974 *J. Non-Met.* **2** 95
[14] Carini G, Cutroni M, Fontana A, Mariotto G and Rocca F 1984 *Phys. Rev.* B **29** 3567
[15] Swenson J, Borjesson L and Howells W S 1995 *Phys. Rev.* B **52** 9310
[16] Bartolotta A, Carini G, D'Angelo G and Tripodo G 1998 *Solid State Ion.* **105** 97
[17] Abramo M C, Carini G and Pizzimenti G 1988 *J. Phys. C: Solid State Phys.* **21** 527
[18] Chryssikos G D, Duffy J A, Hutchinson J M, Ingram M D, Kamitsos E I and Pappin A J 1994 *J. Non-Cryst. Solids* **172–174** 378
[19] Böhmer R, Ngai K L, Angell C A and Plazek D J 1993 *J. Chem. Phys.* **99** 4201
[20] Kodama M and Kojima S 2002 *J. Therm. Anal. Calorimetry* **69** 961
[21] Sen R S, Xu Z and Stebbins J F 1998 *J. Non-Cryst. Solids* **226** 29
[22] Akagi R, Ohtori N and Umesaki N 2001 *J. Non-Cryst. Solids* **293–295** 471
[23] Varsamis C-P E, Vegiri A and Kamitsos E I 2002 *Phys. Rev.* B **65** 104203
[24] Bray P J 1999 *Inorg. Chim. Acta* **289** 158
Zhong J and Bray P J 1989 *J. Non-Cryst. Solids* **111** 67
[25] Shelby J E 1983 *J. Am. Ceram. Soc.* **66** 225

[26] Ashcroft N W and Mermin N D 1981 *Solid State Physics* (Philadelphia, PA: Holt Saunders Int Edition) p 487
[27] White G K, Collocott S J and Cook J S 1984 *Phys. Rev.* B **29** 4778
[28] White G K, Birch J A and Manghnani M H 1977 *J. Non-Cryst. Solids* **23** 99
[29] Ota R, Yamate T, Soga N and Kunugi M 1978 *J. Non-Cryst. Solids* **29** 67
[30] Saunders G A, Sidek H A A, Comins J D, Carini G and Federico M 1987 *Phil. Mag.* **56** 1
[31] Sato Y and Anderson O L 1980 *J. Phys. Chem. Solids* **41** 401
[32] Shannon R D 1976 *Acta Crystallogr.* A **32** 751
[33] Carini G, Cutroni M, Federico M and Galli G 1984 *J. Non-Cryst. Solids* **64** 317
Carini G, Cutroni M, Federico M, Galli G and Tripodo G 1984 *Phys. Rev.* B **30** 7219
[34] Carini G Jr, Carini G, Tripodo G, Bartolotta A and Di Marco G 2006 *J. Phys.: Condens. Matter* **18** 3251
[35] Jackle J, Pichè L, Arnold W and Hunklinger S 1976 *J. Non Cryst. Solids* **20** 365
[36] Gilroy K S and Phillips W A 1981 *Phil. Mag.* B **43** 735
[37] Jackle J 1972 *Z. Phys.* **257** 212
[38] Carini G, Cutroni M, Federico M and Tripodo G 1988 *Phys. Rev.* B **37** 7021
[39] Devaud M, Prieur J Y and Wallace W D 1983 *Solid State Ion.* **9/10** 593
[40] Reichert N, Schmidt M and Hunklinger S 1986 *Solid State Commun.* **57** 315
[41] Garber J A and Granato A V 1975 *Phys. Rev.* B **11** 3990
[42] Claytor T N and Sladek R J 1978 *Phys. Rev.* B **18** 5842